ELSEVIER

Journal of Photochemistry and Photobiology A: Chemistry 113 (1998) 35–43

Journal of Photochemistry and Photobiology A:Chemistry

Excited state dynamics of 4(1*H*-pyrrole 1-yl) benzoic acid and different environmental effects

Prakriti Ranjan Bangal [a], Sankar Chakravorti [a,*], Golam Mustafa [b]

[a] *Department of Spectroscopy, Indian Association for the Cultivation of Science, Jadavpur, Calcutta-700032, India*

[b] *Department of Solid State Physics, Indian Association for the Cultivation of Science, Jadavpur, Calcutta-700 032, India*

Received 12 June 1997; received in revised form 22 August 1997

Abstract

The absorption and fluorescence characteristics of 4(1*H*-pyrrole 1-yl) benzoic acid (PBA) in solvents of different polarities, acidities, glass matrices and also in β-cyclodextrin cavity were studied with regard to the influence of flexibility of the molecule in both the ground and excited sates. The study of dynamics of excited state reveals the presence of two competitive fluorescence emission from a common excited state of PBA. Of these two fluorescence bands one originates from delocalized excited (DE) state [i.e., Franck–Condon (F–C) excited state] and the other from twisted intramolecular charge transfer (TICT) state. The excitation of ground state of PBA leads to the immediate formation of F–C excited state and the TICT state is formed within 220 ps from the parent F–C excited state. The 220 ps time has also been interpreted as the time required for the molecule to relax by rotational motion along the C–N bond of PBA to achieve the TICT state. The steady state photophysical measurements show that the molecule is very weakly fluorescent and nonradiative rate parameters get prominence compared to radiative rate parameters. The fluorescence and phosphorescence studies at 77 K have also been reported. Quantum chemical calculations of the energies and dipole moments were performed for planar and different twisted conformations to confirm experimental findings qualitatively.

Keywords: 4(1*H*-pyrrole 1-yl) benzoic acid; Delocalized excited state; Twisted intramolecular charge transfer state

1. Introduction

Photophysical studies of organic aromatic electron donor/acceptor compounds have led to new information on several issues of contemporary interests, including the role of solvation dynamics in electron transfer reaction and the mechanism of charge transfer process. Intramolecular charge separation is a basic process in chemistry of excited state and the luminescence behavior and it is a powerful mechanism to understand charge separated system. The idea of twisted intramolecular charge transfer state (TICT) by Grabowski et al. [1–3] and Rotkiewicz et al. [4] to explain the anomalous luminescence of 4 *N,N*-dimethyl aminobenzonitrile (DMABN) [5] has given a boost to the quest of new tailor made molecules to be used as fluorescent dyes [6,7], sensing of free volume in polymers [8,9], fluorescence pH or ion indicators [10,11], fluorescent solar collectors [6] and electron transfer photochemistry [12,13]. In polar environment the dual fluorescence of these molecules are caused by delocalized excited state (DE) and TICT states. Quite often these TICT states are non emissive in character and acts as intramolecular fluorescence quencher. In DMABN the TICT state is caused by the transfer of electron [1,14] from lone pair π-orbitals of amino nitrogen to the lowest antibonding π orbital of benzonitrile, both orbitals being symmetric in nature. It was found that the introduction of hetero-aromatic system as pyrrole in place of dimethylamino group opens up a new horizon. The most easily ionizable donor orbital possesses anti symmetric nature and calculation shows TICT states involving symmetric orbitals lie 0.5 eV higher in energy than the anti symmetric one [15]. This might be one of the reasons that make pyrrole [16,17] have a strong tendency for TICT formation. The essential evidence on which the concept of TICT state rests are the measurement of dipole moment of the excited state, solvent effect on absorption and emission spectra, temperature effect and measurement of fluorescence lifetime and these are suitably corroborated by quantum chemical calculations [18–20].

Cyclodextrins are cylic oligosaccharides consisting of multiple glucose units to form a cavity in aqueous solution. The ability to form inclusion complexes with smaller molecules which fit into their (5–8) Å cavities have advantageously

* Corresponding author. E-mail: spsc@iacs.ernet.in

1010-6030/98/$19.00
PII S1010-6030(97)00320-1

been used to control the photophysics and photochemistry of guest molecules. TICT emission was found to be enhanced in some cases [21] and also quenched [22] in other cases inside the cavity. People have attributed the change of emission behavior to nonpolarity of the cavity or to restrictive environment [23–26].

In a preliminary communication [27] TICT state of PBA has been reported. The present paper aims at somewhat extensive photophysical studies of a donor–acceptor system 4(1*H*-pyrrole 1-yl) benzoic acid (PBA) along with quantum chemical calculation with a view to understand the nature of charge transfer due to the pyrrole unit of PBA.

2. Experimental details

The sample 4(1*H*-pyrrole 1-yl) benzoic acid was purchased from Aldrich Chemical, USA and was further purified by recrystallization. The spectral grade solvents, were obtained from Aldrich Chemical, USA (Methylcyclohexane, MCH), or from E. Merck (Cyclohexane, CH; Acetonitrile, ACN; Methanol, MeOH; Ethanol, EtOH; *N,N*-dimethyl formamide, *N,N*-DMF and chloroform, $CHCl_3$) and were used after vacuum distillation. All the solvents were checked for absence of any fluorescence emission in the wavelength region of interest prior to preparing the solution. Absorption spectra were recorded with a Shimadzu absorption spectrophotometer, model UV-2101 PC with the solution concentration less than 10^{-4} M using 1 nm band width. The fluorescence emission spectra were recorded with a Perkin Elmer spctrophotometer model MPF-44A. A sample cell with 1 cm optical path length was used in normal 90° configuration at room temperature. Phosphorescence emission spectra were recorded with specially made low temperature attachment of Perkin Elmer spectrophotometer. The phosphorescence lifetime was measured from the decay of the intensity of phosphorescence band on a recorder after the intensity had been achieved [16]. Quantum yields were determined by using the secondary standard method, with recrystalized β-napthol in cyclohexane ($\phi_{fl}=0.3$) as Ref. [28]. Concentrations were adjusted to be below 10^{-5} M in specified solvents with similar absorbance below 0.1 at λ_{ex}. The following equation was applied for calculating the quantum yields.

$$\phi_2 = \frac{\phi_1 A_2(\lambda) n_2^2 \int F_1(\lambda)\mathrm{d}\lambda}{A_1(\lambda) n_1^2 \int F_2(\lambda)\mathrm{d}\lambda}$$

$A(\lambda)$ is the absorption of the solution at λ_{ex} (300 nm), n is the refractive index of the solvent, and the integral $\int F(\lambda)\mathrm{d}\lambda$ is the area under the fluorescence spectrum and suffix 1 refers to β-napthol in cyclohexane (standard) and 2 refers to the PBA in different solvents.

The time resolved fluorescence decay of PBA in ACN was observed by employing a CW mode-locked frequency doubled Nd-YAG laser-driven dye (Rhodamine 6G) laser operating at a repetition rate of 800 kHz with pulse width of the order of 4–10 ps [29]. Fluorescence lifetime in ACN was obtained by using a time-correlated single-photon-counting coupled to a micro channel plate photomultiplier (Model 28090; Hamamatsu). The instrument response function (IRF) was obtained at 295 nm using a dilute colloidal suspension of dried nondairy coffee whitener. The cut-off filter was used to prevent scattering of excitation beam and the emission was monitored at the magic angle (54.7°) to eliminate the contribution from the decay of anisotropy. The fluorescence lifetime in MCH was measured by using single-photon-counting fluorimeter (Edinburgh Instrument, UK) with excitation source N_2-filled nanosecond flash lamp.

For the luminescence study in β-CD cavity, β-CD was used as received from Aldrich Chemical. The sample concentration of the solution in Millipore water was maintained to keep constant (10^{-5} M) for all different β-CD concentrations. Isosbestic points were used to excite the molecule. All fluorescence spectra in β-CD solutions have been recorded with Hitachi Spectrophotometer model F-4500.

3. Results and discussion

3.1. Absorption spectra

The absorption spectra of PBA recorded in different polar and nonpolar solvents at room temperature show strong structureless broad band (Fig. 1) having λ_{max} in the range of (281–290) nm (ν_{max} in the range of $34.56–35.71\times10^3$ cm^{-1}), Table 1. Due to greater stabilization in the ground state energy in more polar and hydrogen bonding solvents the hypsochromic effect of absorption band is observed (Table 1) and

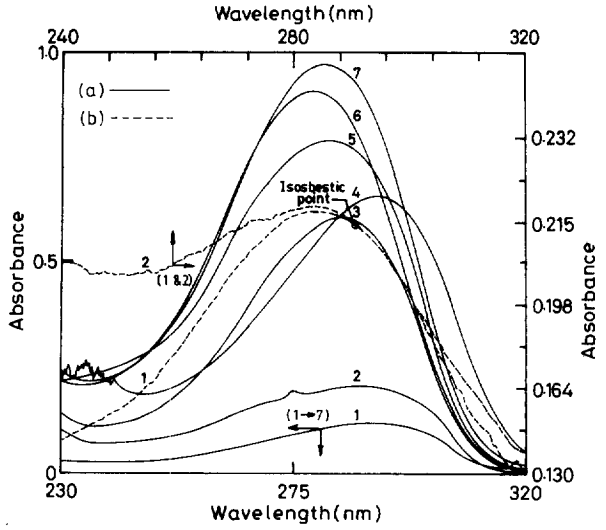

Fig. 1. (a) Electronic absorption spectra of PBA in the concentration range of 10^{-5} M at 300 K in a 1-cm cell in different solvents. (1) MCH, (2) CH, (3) ACN, (4) $ChCl_3$, (5) *N,N*-DMF, (6) MeOH, (7) EtOH. (b) Electronic absorption spectra of PBA in (1) water and (2) water and β-CD ($c=1.36\times10^{-2}$ M) solution at 300 K. Sample concentration ~ 10^{-5} M.

the transition is expected to be $n\pi^*$ one [30]. But the absorptivity of this band ($\varepsilon_{max} \sim 10^4$) resembles the band of $\pi\pi^*$ character. A cursory look at the structure of the molecule gives an impression of possibility of its showing a charge transfer band. So there might be a weak hidden band under strong C–T band and this probably makes the absorption band broad and structureless.

The absorption spectra of PBA in water at room temperature shows a similar type of structureless broad band with λ_{max} at 283 nm ($\nu_{max} = 35.33 \times 10^3$ cm^{-1}) like in other organic solvents. In acidic medium this band showed a large shift to 288 nm but in basic medium no change in λ_{max} was noticed. This red shift of absorption band is due to protonation of pyrrole N atom, and which in turn decreases the necessary conjugation producing spectral shift. Fig. 1b shows the absorption spectra of PBA in pure water and highly concentrated β-CD solution. For all other lower concentrated β-CD solution, the absorption spectra lie between those two spectra with slight increased absorbance. An isosbestic point detected at 286 nm confirms the formation of single equilibrium involving one-to-one complex. In basic solution β-CD makes no change in absorption band but in acidic β-CD solution, PBA shows a bathochromic shift. In this case also an isosbestic point could be observed at 292 nm. For both the cases the slight increase in absorbance may be attributed to the less surface tension of β-CD (detergent effect) solution [31].

3.2. Emission spectra

PBA in different polar solvents exhibits prominent dual fluorescence, consisting of two distinct bands, the anomalous long wavelength A band at about (410–480) nm and short wavelength B at (335–340) nm wavelength region (Table 1). On the other hand, in nonpolar solvent, i.e., in hydrocarbon media PBA shows only one fluorescence band with increased quantum yield (~10 times more) nearly at the same position of the above mentioned (Table 1) B band in polar solvents. This B band corresponds to the normal fluorescence band of benzene $^1B_{2u} \rightarrow {}^1A_{1g}$ transition, which may be ascribed to the delocalized excited state (DE) in phenyl ring and it did not show discernible solvent dependent shift. The both bands of dual fluorescence of PBA in polar aprotic solvent are independent of concentration and excitation wavelength over a large range. The fluorescence intensity is nearly independent in the concentration range of (10^{-5}–10^{-6}) M. The intensity of both bands decrease with increasing concentration and at concentration 2.5×10^{-3} M the dual fluorescence hardly exists. These findings points that at higher concentration PBA forms dimer by hydrogen bonding between acid parts of two molecules. Now to avoid the formation of dimeric form, all fluorescence studies have been confined to the sample concentration less than 10^{-5}M. Fig. 2a shows that the broad structureless anomalous fluorescence A band of PBA having large red shift in solvents of increasing polarity. This polarity effect of A band and the quantitative analysis of this red shift evinces that the corresponding emitting state possesses a large dipole moment [32]. The change of dipole moment from ground state to excited state of the molecule has been worked out in terms of Onsager theory of dielectrics. According to this, the energy shift between 0–0 band in absorption and emission is related to the dielectric constant D and refractive index n of the solvent and the difference in dipole moments ($\mu_e - \mu_g$) or $\Delta\mu$ in two combining energy states has been used to calculate by the following relation [33]

$$\Delta\tilde{\nu} = \frac{2(\mu_e - \mu_g)^2}{hca^3}\left(\frac{D-1}{2D+1} - \frac{n^2-1}{2n^2+1}\right)$$

where a is the radius of the Onsagar's cavity and μ_e and μ_g are the dipole moment in excited and ground state of the molecule respectively. The value of a was estimated from geometrical dimension of the molecule to be 4.2 Å as found from optimized geometry determined by nonlinear least square sub-routine of MOPAC. Using this relation, the calculated $\Delta\mu$ was found to be 12.3 Debye and this large value indicates that band A might have a polar character and this is the intramolecular charge transfer state [34]. The quantum

Table 1
Room temperature absorption and emission data of PBA

Solvent	Absorption data			Fluorescence data					
	λ_{max} (nm)	$\nu_{max} \times 10^{-3}$ cm^{-1}	$\varepsilon_{max} \times 10^{-3}$ M	λ_{max}^B (nm)	$\nu_{max}^B \times 10^{-3}$ cm^{-1}	λ_{max}^A (nm)	$\nu_{max}^A \times 10^{-3}$ cm^{-1}	ϕ_B	ϕ_A
CH	290	34.48	–	340	29.41	–	–	0.220	–
MCH	291	34.36	–	335	29.85	–	–	0.230	–
MeOH	281	35.58	8.5	330	30.30	430	23.25	0.012	0.019
EtOH	284	35.21	8.7	340	29.41	410	24.39	0.013	0.013
ACN	285	35.08	8.7	340	29.41	480	20.83	0.018	0.021
$CHCl_3$	291	34.36	9.26	335	29.85	420	23.81	0.016	0.018
N,N-DMF	281	35.36	10.36	335	29.85	450	22.22	0.020	0.025
Water	283	35.33	–	330	30.30	–	–	0.001	0.0
Water + β-CD (conc.)	284	35.59	–	330	30.30	460	21.74	0.011	0.018

$M = dm^3\ mol^{-1}\ cm^{-1}$.

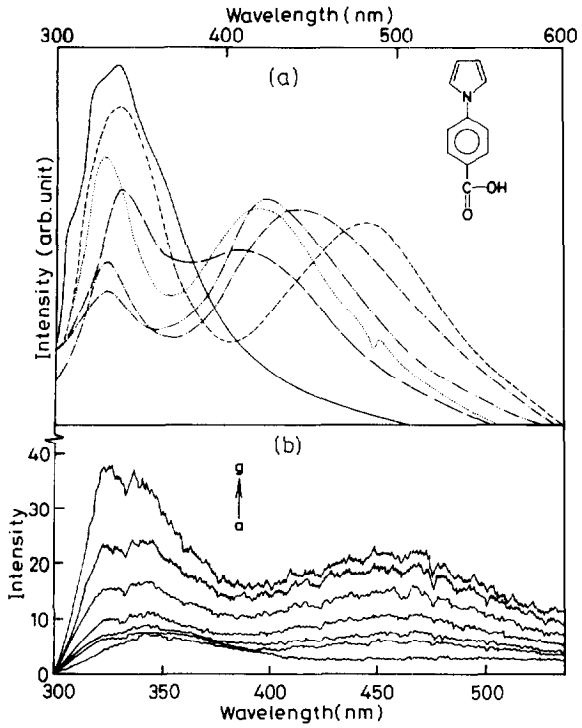

Fig. 2. (a) Fluorescence emission spectra of PBA at room temperature ($c \sim 10^{-5}$ M) in different solvents. (—) MCH, (— · · —) MeOH, (— · —) *N,N*-DMF, (· · ·) $CHCl_3$, (– – –) EtOH and (- - -) ACN ($\lambda_{ex} = 300$ nm). (b) Fluorescence emission spectra of 2×10^{-5} M aqueous solution of PBA in β-CD concentrations (a) 0, (b) 4.2×10^{-4}, (c) 8.5×10^{-4}, (d) 1.7×10^{-3}, (e) 3.4×10^{-3}, (f) 6.8×10^{-3}, (g) 1.36×10^{-2} M. ($\lambda_{ex} = 286$ nm and pH = 7).

chemical calculations by MOPAC/s AM1 hamiltonian indicate the value of $\Delta\mu$ to be 5 Debye. Though there is a large difference between calculated and measured $\Delta\mu$ value, yet it confirms qualitatively that, a sufficient amount of dipole moment change occur in excited state as well as in twisted conformer, which is associated with large redistribution of charges in above said situations.

In pure water solution PBA shows a little trace of B band emission and practically no A band emission, but in the presence of β-CD in water solution PBA shows strong dual fluorescence when excited by 286 nm wavelength, the isosbestic point of absorption spectra Fig. 1b. Fig. 2b shows the fluorescence spectra of PBA as a function of β-CD concentration. With increase of β-CD concentration the DE band (B band) and A band are enhanced, and both the bands are shifted to the blue while the DE band is found to be resolved a bit showing vibronic structures. In basic medium the characteristics of the spectral behavior in presence of β-CD are the same, but those dramatically change in acidic medium with β-CD. In this medium, water solution of PBA produce neither B band nor A band. But, addition of β-CD in the acidic water solution of PBA produces only B band fluorescence. With gradual increment of β-CD concentration, B band is well resolved into two peaks at 321 nm and 335 nm (Fig. 2b). All these fluorescence characteristics in both acidic and basic medium evince the formation of PBA. β-CD inclusion complex, as it was found in absorption spectra (vide supra). Now as the guest (PBA) molecule is engulfed into the host, the chromophores are protected from collision, which could be the reason of the resolution of B band in presence of β-CD concentration.

The above mentioned results may be rationalized by the existing knowledge of TICT [7,35,36] process. On electronic excitation, a bichromophoric molecule containing an electron donor and an electron withdrawing group, an ICT* state with partial electron transfer is formed initially. With an increase in solvent polarity, the ICT* states are sufficiently solvated, which decreases the energy gap between the ground and excited state resulting in the red shift of ICT* emission. In polar media, the pyrrole ring of PBA takes up a twisting position which makes donor orbital perpendicular to the acceptor making minimum overlap of π-orbital and which leads to TICT state. With the increase in polarity of the medium, the transition state for TICT process is stabilized to a greater extent than ICT* state. Also, the inclusion of a carboxyl group in acceptor moiety increases the electron withdrawing capacity of the phenyl ring, which enhances charge transfer character from the donating moiety of PBA, thereby markedly accelerating the TICT process. Since TICT is the main nonradiative process in ICT* states, PBA shows lower quantum yield in polar media than nonpolar media. Hence we can assign the second anomalous fluorescence band of dual fluorescence, i.e., A band to TICT band. As the excitation spectra of both the bands A and B of PBA are identical (Fig. 3) in their structure and also the excitation spectrum of B band is identical to the absorption spectra of PBA it may be concluded clearly that A and B bands arise from the same Franc–Condon excited state. This is an added proof for the assignment of A band as TICT band.

Water, being a highly polar solvent has the ability to stabilize the TICT state a lot and lowering its energy level. This will in turn increase the nonradiative decay of the TICT state [21,22] and thereupon cessation of TICT band emission. When β-CD is added to neutral and basic solution, the encapsulated sequestered guest molecule PBA faces less polar environment [37]. As a result the TICT state does not get sufficiently stabilized by solvation and the energy gap between TICT state and the low lying triplet or ground state

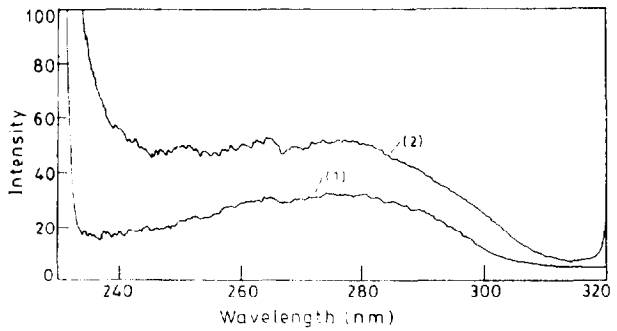

Fig. 3. Fluorescence excitation spectra of PBA in aqueous β-CD solution at 300 K. (1) $\lambda_{em} = 340$ nm and (2) $\lambda_{em} = 460$ nm, pH = 7.

is increased showing the blue shift and intense dual fluorescence. Again, the β-CD cavity may have some geometrical constraint, which decreases the rotational freedom of the flexible part of the host molecule in the excited state. The TICT excited state is probably achieved through the orthogonal position between two different π systems of the molecule which is transition forbidden [38]. Owing to reduced rotational freedom inside the cavity, two different π-systems of the molecule might not be in a perpendicular position in the excited state. This reduction of perpendicularity condition in the excited state thereupon increases the transition probability and enhancement of the A band. Another interesting feature was observed that in the excitation spectrum, the intensity of λ_{max} corresponding to the TICT band is higher than that of the DE band (Fig. 3). The intensity ratio I_A^{ex}/I_B^{ex} of the excitation spectra was the same as the ratio I_A/I_B emission spectra keeping the excitation wavelength the same for both the A and B bands. This result not only confirms the 1:1 complex formation between host and guest but also confirms a relationship between DE and TICT state. From the aforesaid results of PBA in acidic solution in the presence of β-CD, it is established that, the electron rich pyrrole ring looses its donating strength due to protonation and no TICT emission could be observed even with increased β-CD concentration in solution, whereas the DE emission remains the same. In this case, the sequestered guest molecule in the cavity behaves like a benzene derivative. Generally, the excited states of benzene derivatives having the NH group are efficiently quenched by water molecule [39]. So the enhancement of the B band emission may be due to the elimination of water molecules surrounding the fluorescent molecule due to insertion of the molecule in the cavity.

3.3. Temperature effect on dual fluorescence

In acetonitrile solvent the intensity of A band fluorescence increases with increasing temperature in the range of 283 K–338 K while the intensity of B band fluorescence decreases (Fig. 4). The intensity ratio I_A/I_B increases in this temperature range. So it is clear that, the enhancement of A band is performed at the cost of B band intensity. Now as we go down to 77 K in both polar and nonpolar glass matrices, PBA exhibits only the B band fluorescence with moderately high quantum efficiency (Table 2). Interestingly, the A band fluorescence starts to appear in the temperature range of 152 K to 154 K while the B band starts to loose its intensity. Hence it may be concluded that the B band is responsible for the birth of A band fluorescence. At the temperature range 152 K–154 K probably the super-cooled matrix offers less resistance to the rotation of the flexible part of PBA. All these foregoing discussions point to the fact that essentially, the A band arises due to TICT, the necessary twist might be possible around the single bond connecting the donor (pyrrole) and the acceptor moieties for the TICT state.

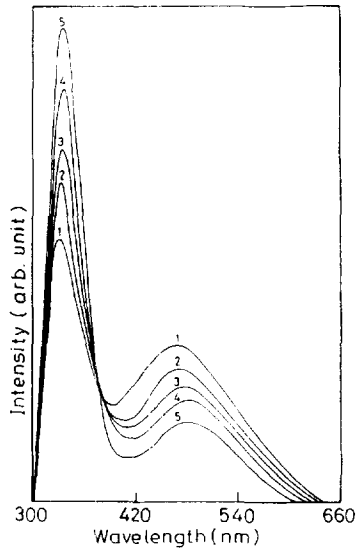

Fig. 4. Temperature dependence of fluorescence emission spectra of PBA in acetonitrile solvent. (1) 338 K, (2) 323 K, (3) 313 K, (4) 303 K, (5) 293 K (λ_{ex} = 300 nm).

Table 2
Emission data at 77 K

Solvent	λ_{max}^{fl} (nm)	$\nu_{max}^{fl} \times 10^{-3}$ cm^{-1}	λ_{max}^{P} (nm)	$\nu_{max}^{P} \times 10^{-3}$ cm^{-1}	ϕ_{fl}	ϕ_P	τ_P (s)
MCH	340	29.41	405	24.69	0.2	0.17	2.4
			435	22.99			
EtOH	340	29.41	400	25.00	0.3	0.2	2.1
			430	23.25			

3.4. Luminescence of PBA at 77 K

At 77 K, PBA shows only the normal fluorescence band B with very significant quantum yield (Table 2) in both polar and nonpolar glass matrices and in addition to this it shows strong phosphorescence band in the wavelength region of TICT (A) band. So this system with singlet/triplet nearly degenerate pair in excited state may be called biradicaloid. At 77 K the possibility of relaxation and twist of pyrrole ring to 90° is very unlikely to happen, so the phosphorescence from unrelaxed tripled should be observed. The analysis of phosphorescence spectra apparently lead some contradiction regarding the character of triplet from the following observations. Firstly, the tendency of the phosphorescence quantum yield to be higher while going from MCH to EtOH (Table 2). Secondly, the phosphorescence (0,0) band shows large hypsochromic shift (310 cm^{-1}) as we go from MCH to ethanolic glass (Fig. 5, Table 2). In view of the above characteristics of phosphorescence band, the nature of the triplet state may be assigned to be $n\pi^*$, on the other hand the lifetime of the triplet states (2 s) is too large to qualify for an $n\pi^*$ state. Again the phosphorescence in ethanol glass is

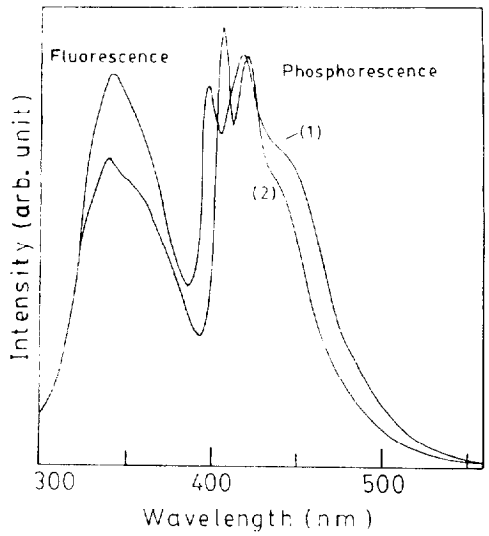

Fig. 5. Fluorescence and phosphorescence emission spectra of PBA at 77 K in different glass matrices. (1) EtOH, (2) MCH. (λ_{ex} = 300 nm).

governed by hydrogen bonding interactions which alter the band width and the vibrational fine structure of $\pi\pi^*$ transitions. In this context it may be mentioned that the pure $n\pi^*$ or $\pi\pi^*$ triplet state is unexpected and mixing of two states through the vibronic coupling [40,41] may not be ruled out.

4. Origin of dual fluorescence

The fluorescence decay data for the DE state (λ_{max} = 340 nm) i.e., B* state and TICT state (λ_{max} = 480 nm) i.e., A* state is measured in acetonitrile solvent. The B band fluorescence decay is resolved into two exponential components (Fig. 6). The first component decay with lifetime and amplitude of 220 ps ± 10 ps and 0.6, respectively and the second is the slower component composed of lifetime of 1.37 ns ± 0.2 ns. The A band fluorescence has monoexponential decay with a lifetime of 1.28 ns ± 0.2 ns (Fig. 7) which follows the decay time of the slower component of B band fluorescence. Hence it is clear that the fast component with decay time 220 ps ± 10 ps is the rise time of the A band (TICT) fluorescence. The fluorescence decay data for the DE state, i.e., B* state is also measured in MCH solvent, where the very slower monoexponential decay is observed with lifetime 3.2 ns. The fluorescence lifetime ratio of DE state in MCH to ACN is 2.5, whereas the quantum yield ratio of DE state fluorescence in these same solvents is nearly 10. This discrepancy suggests that the population of TICT state (A* state) in ACN originates from DE state (B* state) at the cost of population of the B* state and hence low quantum yield result of B band emission in ACN. These findings confirm that an equilibrium is rapidly established between the states responsible for B band fluorescence and A band fluorescence.

This equilibrium may be expressed as

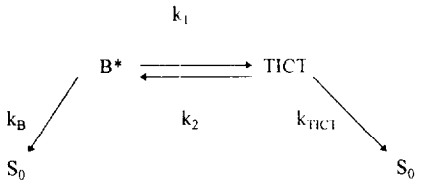

where B* represents the state responsible for normal B band (DE state) fluorescence and TICT represents the state responsible for A band fluorescence, and k_B, and k_{TICT}, are the radiative and nonradiative decay rate for B* and TICT respectively, and k_1 and k_2 are the forward and backward rate constants. After pulse excitation, the decay of two states can be described as

$$\frac{d[B^*]}{dt} = -(k_1 + k_B)[B^*] + k_2[TICT]$$

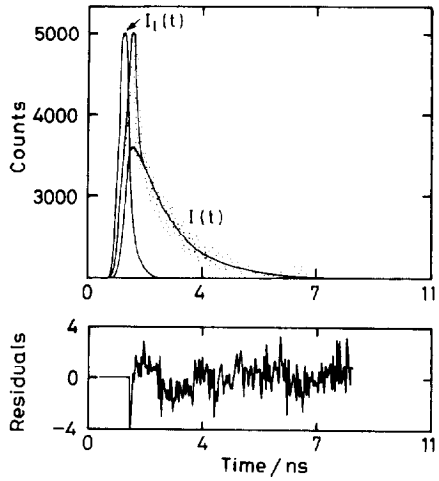

Fig. 6. Fluorescence decay profile $I(t)$ of PBA in ACN excited at 300 nm and monitored at 340 nm. $I_1(t)$ is the lamp function. τ_1 = 0.22 ns (60%), τ_2 = 1.37 ns (40%) and χ^2 = 1.1.

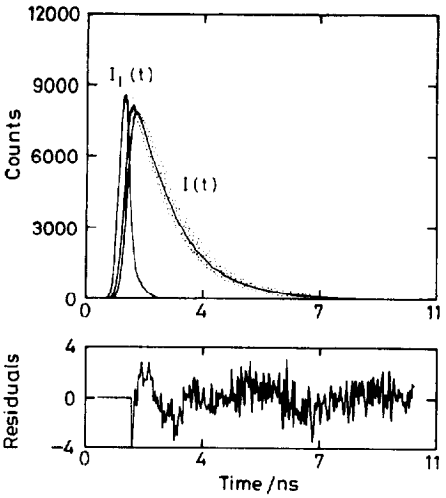

Fig. 7. Fluorescence decay profile $I(t)$ of PBA in ACN excited at 300 nm and monitored at 480 nm. $I_1(t)$ is the lamp function. The fluorescence decay time τ = 1.28 ns and χ^2 = 1.1.

Table 3
Excited state depletion rate parameters at room temperature

Solvent	τ_f^B (ns)	τ_f^{TICT} (ns)	$k_r^B \times 10^{-8}$ (s^{-1})	$k_{nr}^B \times 10^{-8}$ (s^{-1})	$k_r^{TICT} \times 10^{-8}$ (s^{-1})	$k_{nr}^{TICT} \times 10^{-8}$ (s^{-1})
MCH	***3.2***	–	***0.7***	***2.4***	–	–
ACN	***1.37***	***1.28***	***0.16***	***7.4***	***0.15***	***7.7***
ACN	1.21	1.49	0.149	8.13	0.14	6.57
MeOH	1.26	0.786	0.15	7.8	0.14	12.16
EtOH	1.12	0.866	0.16	8.7	0.15	11.4
$CHCl_3$	1.05	1.00	0.17	9.4	0.16	9.8
N,N-DMF	1.315	1.11	0.19	7.4	0.18	8.8

Bold and italic fonts indicate the data from measured fluorescence lifetime and quantum yield.

$$\frac{d[\mathrm{TICT}]}{dt} = -(k_2 + k_{\mathrm{TICT}})[\mathrm{TICT}] + k_1[\mathrm{B}^*]$$

The standard solution of these equations are

$$I_B(t) = \frac{I_0}{\lambda_2 - \lambda_1}[(\lambda_2 - k_B - k_1)e^{-\lambda_1 t} + (k_B + k_1 - \lambda_1)e^{-\lambda_2 t}]$$

and

$$I_{\mathrm{TICT}}^{(t)} = \frac{I_0}{\lambda_2 - \lambda_1}[e^{-\lambda_1 t} - e^{\lambda_2 t}]$$

where

$$\lambda_1(\lambda_2) = \frac{1}{2}[(k_B + k_1 + k_{\mathrm{TICT}} + k_2) \mp ((k_{\mathrm{TICT}} + k_2 - k_B - k_1)^2 + 4k_1k_2)^{1/2}]$$

I_B and I_{TICT} are the fluorescence intensities for B* and TICT respectively. So B* will now show exponential decay with lifetimes $1/\lambda_1$ and $1/\lambda_2$ and the fluorescence of TICT state will have an exponential rise with lifetime $1/\lambda_2$ exponential decay with life time $1/\lambda_1$. The experimental observations produce $1/\lambda_2 = 220\ \mathrm{ps} \pm 10\ \mathrm{ps}$ and $1/\lambda_1 = 1.37\ \mathrm{ns} + 0.2\ \mathrm{ns}$. For fast equilibration rate the expression for λ's reduces as

$$\lambda_2 \approx k_1 + k_2 \text{ and } \lambda_1 \approx k_B + k_{\mathrm{TICT}}$$

So the measured fast lifetime 220 ps represents the sum of forward and backward equilibration rate while the long lifetime 1.37 ns represents the sum of other radiative and nonradiative decay channels.

The radiative and nonradiative rate constants of PBA have been calculated for MCH and ACN solvent from fluorescence decay time and fluorescence quantum yield using the following equations

$$k_r = \frac{\phi_{fl}}{\tau_{fl}} \text{ and } k_{nr} = \frac{(1 - \phi_{fl})}{\tau_{fl}}$$

Again these radiative rate constant also has been calculated by using simplified form of Strickler and Berg equation [42].

$$k_r = 1.713 \times 10^5 \varepsilon_a$$

Fortunately the value of radiative rate constant from fluorescence and that from absorption through Strickler and Berg equation are in same order although this equation is not suitable for this case where the molecular geometry is changed in excited state. Similarly, the radiative and nonradiative rate constant of different states have been calculated for other solvents (Table 3).

5. Quantum-chemical calculation

In order to have a better qualitative understanding of different excited state properties, the energies of electronic transitions and dipole moments were calculated by using AM1 hamiltonian embeded in MOPAC/s CI(4×4) method [18–20] for PBA in ground and excited states considering the planar conformer as well as different twisted conformers. A CI calculation involves the interaction of microstates representing specific interaction of electrons in a set of molecular orbitals including the highest occupied and lowest unoccupied molecular orbitals, starting with a set of electronic configuration. The molecular coordinates were generally obtained from minimum energy geometries determined by a PC model molecular modeling software (DTMM).

In order to observe the anomalous fluorescence (TICT emission), a sufficient energy lowering of the ^{1}A excited state should take place. Solvent relaxation may be responsible for bringing the ^{1}A state close to or below ^{1}B, which is the lowest excited state for the nonrelaxed system (^1L_b). The proximity of the ^{1}B and ^{1}A states can play an important role in the possible energetic reversal of these two states due to polar solvent effect.

From CI(4×4) calculations we find the energy difference (ΔE) between the ^{1}A and ^{1}B is very low in flat geometry, i.e., for planar conformation. Fig. 8 shows the variation of ground state, ^{1}A and ^{1}B state with twist angle around the C–N bond. The twist of pyrrole ring around the C–N bond is energetically favourable for excited ^{1}A state while the energy of the ^{1}B state rises with twisting of pyrrole ring. In flat geometry two states are very close and in 20–30° twisting position of pyrrole ring there is a surface crossing (Fig. 8). These findings confirm that in polar solvent the state reversal is achieved by intramolecular/solvent relaxation. The energy

Table 4
Dependence of the energy E (wavelength) and dipole moment of the lowest electronic transitions (S_1–S_0), (S_2–S_0) and (T_1–S_0) on twist angle θ of pyrrole ring around C–N bond

Angle θ°	(S_1–S_0) ΔE (eV)	(S_1–S_0) λ_{max} (nm)	(S_2–S_0) ΔE (eV)	(S_2–S_0) λ_{max} (nm)	(T_1–S_0) ΔE (eV)	(T_1–S_0) λ_{max} (nm)	μ (Debye)
0	3.795	327	3.85	323	3.74	332	6.79
10	3.795	327	3.84	323	3.73	333	6.83
20	3.795	327	3.81	326	3.71	334	6.94
30	3.795	327	3.76	330	3.66	339	7.09
40	3.810	326	3.69	336	3.60	345	7.31
50	3.832	324	3.61	344	3.51	354	7.52
60	3.944	315	3.50	355	3.2	388	7.72
70	4.010	309	3.30	376	3.2	388	7.81
80	3.782	328	3.56	349	3.51	354	8.51
90	3.651	340	3.61	344	3.56	359	8.31

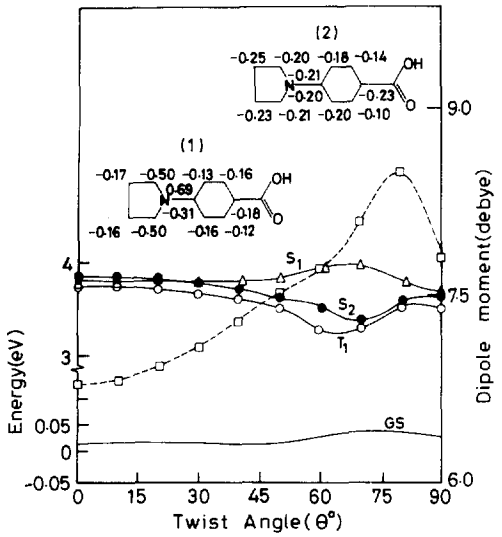

Fig. 8. Plot of ground state, first, second excited singlet and triplet state energy of PBA against twist angle θ around C–N bond. (1) charge distribution of PBA in excited state (twisted angle $\theta = 0^\circ$), (2) Charge distribution of PBA in excited state (twisted angle $\theta = 80^\circ$). The benzene ring bond lengths are $l_{C\text{-}C} = 1.4$ Å, $l_{C\text{-}H} = 1.1$ Å. The pyrrole ring bond lengths are $l_{C\text{-}C} = 1.39$ Å, $l_{C\text{-}H} = 1.08$ Å, $l_{C\text{-}N} = 1.4$ Å. The other bond length are $l_{C\text{-}O} = 1.23$ Å, $l_{O\text{-}H} = 0.96$ Å, $l_{C\text{-}O} = 1.37$ Å. Plot of dipole moment (- - -) of PBA in excited state against twist angle θ around C–N bond.

minimum for first excited state (^{1}A) appears around 60°–70° twisted position and the twist around the C–N bond causes a strong charge separation in ^{1}A state. The charge difference on N-atom ($\Delta q = 0.5$ e) between planar and twisted conformer in excited state ^{1}A is larger than that of in ground state (Fig. 8) between the two said conformers ($\Delta q = 0.04$ e). A small rotational barrier could be found as the ground state energy changes with angle of twist around C–N bond. This confirms that, in the ground state a planar structure is favoured which is also evident from the optimized geometry of PBA by MOPAC. The triplet state energy calculations by configuration interaction show an energy minimum like singlet state on twisting the two chromophores around the C–N bond (Fig. 8). The interesting feature here is that the lowest triplet state corresponding to the planar geometry is very close to the first excited singlet ^{1}A state in twisted geometry. So the singlet and triplet are degenerate in nature and the charge transfer may be termed as 'biradicaloid charge transfer' [43].

Fig. 8 depicts the variation of excited state dipole moment with the angle of twist around the C–N bond. The ground state dipole moment of PBA is calculated to be 3.54 Debye and it is invariant for all possible angle of twist around the C–N bond. The maximum change of dipole moment from ground to excited state was found to be 5 Debye in twisted (60°–70°) conformation (Table 4) which itself indicates the major charge redistribution in the twisted form.

The expected mechanism of dual fluorescence of PBA may be through energetically advantageous intramolecular relaxation involving the twisting of phenyl and pyrrole rings around the C–N bond. On excitation, the planar molecule achieves a delocalized excited state and then relaxes to twisted geometry (singlet or triplet), the charge transfer here is biradical in nature and highly polar. Obviously, the emission from the twisted conformer will have a large stokes shift (5000 cm^{-1}) and also be sensitive to environment effect (Table 1) due to large dipole moment change ($\Delta\mu$). The different calculated values of energies, dipole moments along with the corresponding experimental values have been summarized in Table 4.

6. Conclusion

Solvent polarity dependent absorption and emission properties of PBA evinces that, the molecule contains two parallel states in the excited state and one of them has a charge transfer character. Observations recorded in aqueous β-CD solution lead to the conclusion that the anomalous fluorescence is due to twisted intramolecular charge transfer state. Time resolved experiment provides compelling evidence that anomalous (TICT) fluorescence originates from B* state within 200 ps and then decay with nearly the same lifetime as that of the B* state. Finally, quantum chemical calculation energetically

confirms that the twisted configuration of the pyrrole ring of PBA has a lower singlet as well as triplet state.

Hence, from all above observations we can conclude that when the PBA molecule is excited it achieves F–C excited state (B* state) immediately and within 200 ps it also achieves TICT state, which is the major route of depletion through nonradiative transition in polar environment.

Acknowledgements

The help rendered by Chemical Physics group at T.I.F.R., Mumbai and Dr. S. Basak, S.I.N.P, Calcutta in picosecond and nanosecond fluorescence lifetime measurements, respectively, is gratefully acknowledged. The authors also thank Prof. P.K. Mukherjee, IACS for making the software (MOPAC programme) and the computer available to them. The authors would also like to express their sincere thanks to the reviewer for making helpful criticisms and constructive suggestions toward the improvement of the paper.

References

[1] Z.R. Grabowski, K. Rotkiewicz, A.D. Siemiarczuk, J.D. Cowley, W. Bauman, Nouv. J. Chim. 3 (1979) 443.
[2] Z.R. Grabowski, K. Rotkiewicz, W. Rubaszewska, E. Kirkor-Kaminska, Acta. Phys. Pol. A: 54 (1978) 767.
[3] Z.R. Grabowski, K. Rotkiewicz, A. Siemiarczuk, J. Lumin. 18 (1979) 420.
[4] K. Rotkiewicz, Z.R. Grabowski, A. Krowczynski, W. Kuhnle, J. Lumin. 1 (1976) 877.
[5] E. Lippert, W. Lüder, H. Boos, in: A. Mangini (Ed.), Advances in Molecular Spectroscopy, Vol. 1, Pergamon, Oxford (1962) p. 443.
[6] W. Rettig, Nachr. Chem. Tech. Lab. 39 (1991) 298.
[7] W. Rettig, Angew. Chem., Int. Ed. Engl. 25 (1986) 971.
[8] K.A. Al-Hassan, W. Rettig, Chem. Phys. Lett. 126 (1986) 273.
[9] W. Rettig, R. Fritz, J. Springer, in: Photochemical Processes in Organished Molecular Systems, Elsevier, Amsterdam (1993) p. 61.
[10] W. Rettig, Fluorescence Spectroscopy, New Methods and Application, OS, Springer, Berlin (1993) p. 31.
[11] P. Plaza, N.D. Jung, M.M. Martin, Y.H. Meyer, M. Vogal, W. Rettig, Chem. Phys. 168 (1992) 365.
[12] J.L. Habib Jiwan, J.P. Soumillion, J. Photochem. Photobiol. A: Chem. 64 (1992) 145.
[13] J.P. Soumillion, Topics in Current Chemistry, Springer, Berlin (1993).
[14] K. Rotkiewicz, K.H. Grellmann, Z.R. Grabowski, Chem. Phys. Lett. 19 (1973) 315.
[15] W. Rettig, Proc. Indian Acad. Sci. (Chem. Sci.) 104 (1992) 89.
[16] A. Sarkar, S. Chakraborti, Chem. Phys. Lett. 235 (1995) 195.
[17] W. Rettig, F. Marchner, Nouv. J. Chim. 7 (1985) 425.
[18] J.J. Stewart, MOPAC Program 455, Quantum Chemistry Program Exchange, University of Indiana, Bloomington, IN.
[19] M.J.S. Dewar, E.G. Zoebisch, E.F. Healy, J.J.P. Stewart, J. Am. Chem. Soc. 107 (1985) 1765.
[20] M.J.S. Dewar, E.G. Zoebisch, E.F. Healy, J.J.P. Stewart, J. Am. Chem. Soc. 107 (1985) 3902.
[21] Y.B. Jiang, J. Photochem. Photobiol. A Chem: 88 (1995) 109.
[22] A. Nag, K. Bhattacharyya, Chem. Phys. Lett. 151 (1988) 474.
[23] S. Monti, L. Flamigini, A. Martelli, P. Bortolus, J. Phys. Chem. 92 (1988) 4447.
[24] K. Kasatani, M. Kawasaki, H. Sati, J. Phys. Chem. 88 (1984) 5451.
[25] R.A. Agbaria, R. Uzan, D. Gill, J. Phys. Chem. 93 (1989) 3855.
[26] D.W. Cho, Y.H. Kim, S.G. Kang, M. Yoon, J. Phys. Chem. 98 (1994) 558.
[27] P.R. Bangal, S. Chakravorti, Indian J. Phys. 70B (1996) 5.
[28] I.B. Berlman, in: Hand Book of Fluorescence Spectra of Aromatic Molecules, Academic Press, New York (1965) p. 114.
[29] N. Periasamy, S. Doraiswamy, G.B. Maiya, B. Vankataraman, J. Chem. Phys. 88 (1988) 1638.
[30] K.K. Rohatgi-Mukherjee, in: Fundamentals of Photochemistry, Wiley Eastern, New Delhi (1978) p. 102.
[31] G. Wenz, Angew. Chem., Int. Ed. Engl. 33 (1994) 803.
[32] W. Rettig, J. Mol. Struc. 84 (1982) 303.
[33] P. Suppan, J. Photochem. Photobiol. A: Chem. 50 (1990) 293.
[34] H. Shizuka, Pure Appl. Chem. 65 (1993) 1635.
[35] A. Nag, K. Bhattacharyya, Chem. Phys. Lett. 169 (1990) 12.
[36] D. Gormin, M. Kasha, Chem. Phys. Lett. 153 (1988) 574.
[37] M. Hoshino, M. Imamuro, K. Ikehara, Y. Hama, J. Phys. Chem. 85 (1981) 1820.
[38] A. Nag, R. Dutta, N. Chattopadhyay, K. Bhattacharyya, Chem. Phys. Lett. 157 (1989) 83.
[39] K. Bhattachryya, M. Chowdhury, Chem. Rev. 93 (1993) 507.
[40] P.R. Bangal, S. Lahiri, S. Kar, S. Chakravorti, J. Lumin. 69 (1996) 49.
[41] M.A. El-Sayed, J. Chem. Phys. 38 (1963) 2834.
[42] S.J. Strickler, R.A. Berg, J. Chem. Phys. 37 (1962) 814.
[43] V. Bonačić-Koutecký, J. Michl, J. Am. Chem. Soc. 107 (1985) 1765.